Title	Monolithic electrode for electric double-layer capacitors based on macro/meso/microporous S-Containing activated carbon with high surface area
Author(s)	Hasegawa, George; Aoki, Mami; Kanamori, Kazuyoshi; Nakanishi, Kazuki; Hanada, Teiichi; Tadanaga, Kiyoharu
Citation	Journal of Materials Chemistry (2011), 21(7): 2060-2063
Issue Date	2011-01
URL	http://hdl.handle.net/2433/156364
Right	© Royal Society of Chemistry 2011.
Type	Journal Article
Textversion	author

Monolithic Electrode for Electric Double-Layer Capacitors Based on Macro/meso/microporous S-Containing Activated Carbon with High Surface Area

George Hasegawa, [a] Mami Aoki, [b] Kazuyoshi Kanamori, *[a] Kazuki Nakanishi,[a] Teiichi Hanada,[a] Kiyoharu Tadanaga[b]

Macro/meso/microporous carbon monoliths doped with sulfur have been prepared from sulfonated poly(divinylbenzene) networks followed by the activation with CO_2 resulted in the activated carbon monoliths with high surface area of 2400 m^2 g^{-1}. The monolithic electrode of the activated carbon shows remarkably high specific capacitance (175 F g^{-1} at 5 mV s^{-1} and 206 F g^{-1} at 0.5 A g^{-1}).

Increasing demands for the electrochemical devices, such as batteries,[1] fuel cells,[2] and electric double-layer capacitors (EDLCs),[3-6] has triggered the development of porous carbon materials. The physical properties of carbon materials, including surface area, pore volume and pore size, must be controlled to be suitable for each application, because they are closely related to the electrochemical performance. A practical polarized electrode material for EDLCs is activated carbon with a high specific surface area[7-9] because EDLCs are based on electrostatic interactions, *i.e.* the electric charge is accumulated on an electric double-layer of the polarized electrode, and the electrodes with the higher specific surface area can store higher energy. However, the conventional electrodes consisting of microporous carbon particles or powders are not effective enough because the narrow and disordered pores in-between particles or powders are not suitable for the effective transport of ions to the micropore surfaces. In other words, a certain portion of micropores are inaccessible for ions and remain unused. For the better capacitive characteristics, therefore, it is indispensable for porous carbons to have the well-defined larger pores (mesopores and macropores) in addition to the micropores. The mesopores and macropores facilitate the diffusion of the electrolyte ions in the materials while the micropores can provide abundant adsorbing sites for ions.[7,10,11] Thus, great efforts are focused on the preparation of macro/microporous, meso/microporous, and macro/meso/microporous hierarchically porous carbons for EDLCs.[12-21] Monolithic porous carbons are more advantageous for EDLCs rather than the traditional composite pellet electrodes, since the pellet electrodes are fabricated using a mixture of activated carbon powders and binders, such as polytetrafluoroethylene (PTFE), which lower the electric conductivity, and the electrodes are possibly broken into fragments during the charge-discharge cycles. In addition, there is a possibility

that binders unfavorably cover and fill the pores of the activated carbons. Meanwhile, monolithic carbons with continuous skeletons can reduce the internal resistance of the electrode because no binders are needed and all of the pores should remain open and accessible. Hence, the porous carbon monoliths with high surface area are expected to possess the large capacity and show good cycle characteristics. However, there has been very few reports on monolithic EDLCs[12] because it is difficult to obtain porous carbon monoliths with high surface area which are suitable to EDLCs.

Recently, we have reported that macroporous carbon monoliths are successfully prepared from macroporous poly(divinylbenzene) (PDVB) networks, which were fabricated by organotellurium-mediated living radical polymerization (TERP) accompanied by spinodal decomposition.[22,23] Macroporous PDVB monoliths have a significant advantage in the independent controllability in macropore volume as well as in macropore size by simply varying the amount and the molecular weight of polydimethylsiloxane (PDMS), which has not been reported in the conventional phenolic resin monoliths such as resorcinol-formaldehyde so far. We have also reported that the sulfonation of PDVB networks suppresses the shrinkage during carbonization and allows mesopores in the walls of the macropores to be retained even after carbonization.[24] In addition, the carbons prepared from the sulfonated PDVB still contain a small amount of sulfur in their polyaromatic structures. The following activation process by CO_2 imparts high surface area with > 2000 m^2 g^{-1} to the macro-/mesoporous carbon monoliths. In this work, macro/meso/microporous S-doped carbon monoliths with high surface areas are prepared from PDVB networks and are characterized as a monolithic electrode for EDLC. Although there are some reports on the electrodes of N-doped carbons showing a superior capacitance to those of undoped carbons,[25-27] there are no reports on S-doped carbons for EDLCs except for sulfur-functionalized carbon aerogels used as receptor sites of metal catalysts.[28] To the best of our knowledge, this is the first demonstration of the monolithic electrode of S-doped carbons for EDLCs.

In this study, macroporous PDVB with high porosity was prepared following our recently-reported method[22] which employs 1,3,5-trimethylbenzene (TMB) as a solvent, PDMS as the phase-separation inducing agent and DVB as a monomer. Living polymerization of DVB by TERP is initiated by 2,2'-azobis(isobutyronitrile) (AIBN) and is promoted by ethyl-2-methy-2-butyltellanyl propionate (BTEE). The high [TMB]/[DVB] ratio and high molecular weight of PDMS (M_w = 60000-65000) are employed to increase the porosity.[22] In a

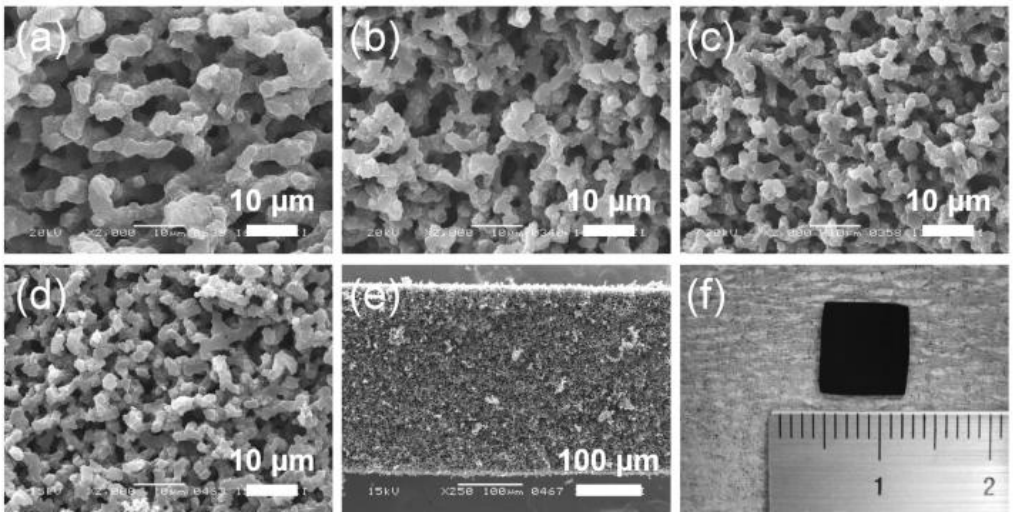

Fig. 1 SEM images of PDVB (a), SPDVB (b), C-1000 (c), and AC-1000 (d). SEM image of the side view (e) and appearance (f) of the AC-1000 electrode for the capacitor.

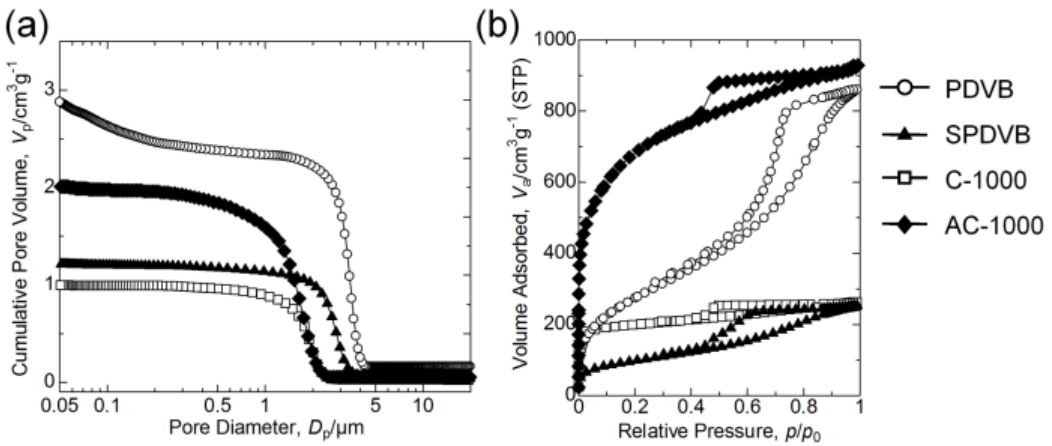

Fig. 2 Pore size distributions (a) and N_2 adsorption-desorption isotherms (b) of the samples, PDVB, SPDVB, C-1000, and AC-1000.

typical procedure, 0.65 g of PDMS was dissolved in a solution containing 5 mL of DVB and 24 mL of TMB. The mixture was stirred at room temperature for 3 min to be homogenized followed by degassing by ultrasonication for 3 min. Then, 0.058 g of AIBN was added to the resultant homogeneous solution and purged with nitrogen supplied using a stainless-steel needle through a silicone resin septum for 10 min. Subsequently, 0.16 mL of BTEE, a promoter of TERP, was injected followed by stirring until AIBN was completey dissolved. The resultant yellow transparent solution was transferred to an ampoule, sealed and kept at 120 °C for 48 h to allow gelation by living polymerization. The obtained wet gels were washed with tetrahydrofuran (THF), followed by drying at 60 °C. After

drying, the macroporous PDVB was sulfonated with conc. H_2SO_4 (the sulfonated sample is denoted as SPDVB) at 150 °C for 24 h in order to inhibit the shrinkage during carbonization as low as possible.[24] The sulfonation of PDVB networks also prevents the monoliths from cracking during carbonization. The sulfonated PDVB gels were washed with H_2O until remaining H_2SO_4 was completely removed. The solvent in the sulfonated gels were mixture of N_2/CO_2 stream with N_2 at a rate of 900 mL $min^{-1}$and exchanged with 2-propanol, followed by evaporative drying at 60 °C. After carbonization at 1000 °C for 2 h with a heating rate of 4 °C min^{-1} in the N_2 stream at a rate of 1 L min^{-1}, the obtained macroporous carbon monoliths (denoted as C-1000) were shaped into thin plates (< 1 mm thick) followed by activation in the CO_2 at a rate of 100 mL min^{-1} at 1000 °C for 4 h so that the whole carbon monoliths can be activated as homogeneously as possible. Unlike carbon powders, since only the surface of the monoliths can be exposed to the activation gas, it is of great importance that monolithic carbons were shaped into thin plates in order to allow the effective activation. The shrinkage of the carbon monolith through the activation process was about 10 % and the weight loss was around 55 %, and the resultant activated sample is denoted as AC-1000.

Figure 1 a-d display the the macroporous structure in the saple monoliths observed under a scanning electron microscope (SEM) (JSM-6060S, JEOL, Japan). As reported previously, the PDVB networks with well-defined interconnected macropores can be obtained by living radical polymerization accompanied by spinodal decomposition. The following sulfonation process facilitates the PDVB networks to be carbonized[29] and allows the macroporous structures to be retained, though the macropores shrink to some extent during the sulfonation and carbonization as shown in Figure 1 b and c. The macroporous structures still remain during the activation as shown in Figure 1 d. The activated carbons were then further-shaped into square plates (*ca.* 7 mm × 7 mm × 300 μm) as shown in Figure 1 e and f in order for the electrochemical evaluation.

The pore characteristics of the samples were measured by Hg porosimetry (Pore Master 60-GT, Quantachrome Instruments, USA) and N_2 adsorption-desorption (Belsorp mini II, Bel Japan Inc., Japan) (Figure 2 a and b and Table 1). It is found that the macropore size of AC-1000 was almost half of that of PDVB due to the shrinkage during the sulfonation and carbonizaion processes while keeping the sharp macropore-size distribution and high specific macropore volume (~ 2 cm^3 g^{-1}). As for the micro- and mesopores, both pore volumes largely decreased during the sulfonation. The following carbonization process increased the micropores and decreased the mesopores because the partial pyrolysis of the networks gives rise to micropores

while the mesopores to some extent collpase due to the shrinkage. Without sulfonation, the mesopores are completely collapsed due to the high shrinkage as reported previously.[23,24] The micropores dramatically increased through the activation by CO_2. The specific volume of micropores and mesopores also increased by the activation because the decrease of bulk density by the pyrolysis of carbons. Also, a part of micropores became larger by the activation to the size of mesopores. Opening the closed mesopores inside the macropore skeletons might be one reason. The resultant activated carbon monoliths have remarkably high specific surface area (>2400 $m^2 g^{-1}$) and 76 % of porosity, which was calculated as $100 \times (1 - [\text{bulk density}]/[\text{true density}])$.

The sulfur content in the samples were measured by energy dispersive X-ray spectroscopy (EDS) (JSM-6060S, JEOL, Japan) as shown in Figure S1 in Electronic Supplmentary Information (ESI). It is found that both C-1000 and AC-1000 contain sulfur. The mole percentages of S/C in C-1000 and AC-1000 are 0.64 % and 0.83 %, respectively. Since the ratio of S/C increased after the activation, it is assumed that carbon is more prone to be pyrolyzed than sulfur by the activation with CO_2. The XRD patterns and Raman spectra of C-1000 and AC-1000 are also measured by powder X-ray diffraction (XRD) (RINT Ultima III, Rigaku Corp., Japan) using Cu Kα (λ = 0.154 nm) as an incident beam and by Raman spectroscopy conducted with a laser raman spectrophotometer (RMP-210, Jasco Corp., Japan) as shown in Figure S2 in ESI. It is found from the XRD patterns that the intensity at lower than 20 deg dramatically increased after the activation because of the increased micropores. As for the Raman spectra, in addition to the bands centered at 1350 cm^{-1} and 1600 cm^{-1}

Table 1 Pore characteristics of the samples

Sample	d_{macro} [a] /μm	Bulk density[b] /g cm^{-1}	a_{BET} [c] /m^2 g^{-1}	$V_{meso\text{-}micro}$ [d] /cm g^{-1}	V_{meso} [e] /cm g^{-1}	V_{micro} [f] /cm g^{-1}
PDVB	3.4	0.21	990	1.33	1.22	0.11
SPDVB	2.7	0.66	360	0.390	0.328	0.06
C-1000	1.8	0.52	770	0.405	0.143	0.26
AC-1000	1.7	0.22	2420	1.43	0.662	0.87

[a] macropore diameter obtained by Hg porosimetry. [b] obtained from Hg porosimetry. [c] BET specific surface area obtained by N_2 adsorption-desorption. [d] micro- and mesopore volume obtained by nitrogen absorption isotherms at $p/p_0 = 0.99$. [e] mesopore volume calculated by the BJH method. [f] micropore volume calculated as $V_{meso\text{-}micro} - V_{meso}$.

which are attributed to D and G bands, a weak and broad band is observed between 1030 cm^{-1} and 1160 cm^{-1}. This peak presumably derives from the vibration of sulfur-containing groups such as sulfone, sulfide and sulfonic species.[30,31]

All the electrochemical measurements were performed in a glass cell using a three-electrode arrangement with an Hg/Hg_2SO_4 reference electrode (potential: 0.615 V vs. Normal Hydrogen Electrode (NHE), RE2C, BAS Inc., Japan) and 2 M aqueous H_2SO_4 as an electrolyte at room temperature by Electrochemical Analyzer (Model 660A, ALS Technology Co., Ltd., Japan). The counter electrode was a platinum plate. The activated carbon plate, AC-1000, shaped into *ca.* 7 mm square and 300 μm thick was attached to the platinum plate with carbon paste (DOTITE, FC-404CA, Fujikura Kasei Co., Ltd., Japan) to configure the electrode. After drying at 100 °C for 2 h, the obtained electrode was immersed in the electrolyte *in vacuo* to fill the pores with the electrolyte completely. Cyclic voltammograms at different sweep rates and galvanostatic charge/discharge tests at various current densities between –0.7 and 0.3 V (vs. Hg/Hg_2SO_4) were carried out. Figure 3 displays the performance of the electrochemical cell equipped with the AC-1000 monolithic electrode. Cyclic voltammograms retain a

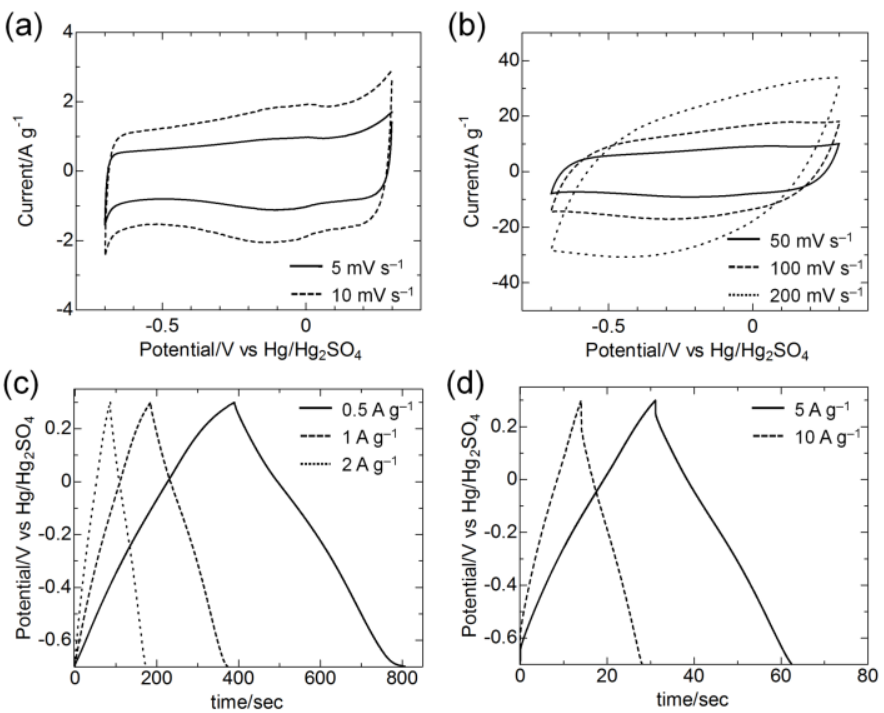

Fig. 3 Electrochemical performances represented by CV curves (a,b) and charge-discharge curves (c,d) for AC-1000 with different scan rates and current densities, measured in 2 M H_2SO_4 aq. using a three-electrode cell.

Table 2 Specific capacitance at different scan rates and current densities.

Scan rate/mV s^{-1}	5	10	50	100	200
Specific capacitance/F g^{-1}	175	166	143	128	103
Current density/A g^{-1}	0.5	1	2	5	10
Specific capacitance/F g^{-1}	206	199	189	177	166

rectangular shape over a wide range of scan rates and the shape did not change to the leaf-like current voltage response even at 100 mV s^{-1}. It is found from the charge and discharge curves that almost no obvious potential drop (IR drop) at the biginning of the discharge process is observed even at 2 A g^{-1} indicating that the thin carbon plate of AC-1000 show high conductivity. The potential of the electrode did not change linearly and the small humps are observed in each curve, which are also observed in cyclic voltammograms, indicating that there presumably is oxidation-reduction relevant to functional groups such as, for example sulfo groups, on the carbon surface.

The obtained specific capacitance values (F g^{-1}) are shown in Table 2. These values have been estimated from the voltammetric charge surrounded by the CV curves according to $C = q/2m\Delta V$, where q, m and ΔV are voltammetric charges on positive and negative sweeps, the weight of cabon, and the potential range of CV, respectively. The capacitance has been also calculated from galvanostatic experiments by using the equation $C = I\Delta t/m\Delta V_d$, where I is the current, Δt is the time spent during the discharge and ΔV_d is the voltage decrease in the discharge. It is found that the electrode of AC-1000 shows remarkably higher specific capacitance even at high scan rate and current density (103 F g^{-1} at 200 mV s^{-1} and 166 F g^{-1} at 10 A g^{-1}) compared to the other activated carbon electrodes reported previously.[32-34] In addition to the hierarchically porous structure which allows effective transport of ions to the carbon surfaces, the monolithic electrode of AC-1000 shows high electroconductivity. These features lead to the high specific capacitance even at high scan rates. In addition, using monolithic electrode, there is no possibility of decreasing the specific surface area of the electrode by an unfavorable filling of pores with binders and by being crushed during milling and pressing. The monolithic

electrodes are also more advantageous when investigating the direct electrochemical responses and performances of electrodes than the traditional composite electrodes.

The stability of capacitance and efficiency with cycling was tested by carrying out cyclic voltammetry with the AC-1000 monolithic electrode between –0.7 V and 0.3 V at 50 mV s^{-1}. The electrochemical cell prepared with AC-1000 showed high stabitily and almost no degradation over 2000 cycles, which suggests that the monolithic electrode keeps the monolithicity and porous structures during the measurement.

In summary, the monolithic carbon electrode for EDLC which has macro-, meso- and micropores and high surface area (>2400 m^2 g^{-1}) has successfully been fabricated from the sulfonated PDVB monolith by carbonization and activation under a 10 % CO_2/N_2 stream at 1000 ºC. The activated carbon still includes small amount of sulfur (S/C = 0.83 % in atomic percent). The small humps are observed in the CV curves and charge-discharge curves, which are presumably attributed to the oxidation-reduction relevant to sulfur-containing groups such as sulfo groups. Further investigation on this phenomenon is currently underway. The resultant monolithic electrode shows high specific capacitance (175 F g^{-1} at 5 mV s^{-1} and 206 F g^{-1} at 0.5 A g^{-1}) and still retains good capacitance even at a high scan rate and current density owing to the hierarchical pore structure which allows an effective transport of ions, and to the high conductivity of the monolithic electrode. In addition, the electrochemical cell prepared with the monolithic activated carbon shows good cycle performance. A new possibility of monolithic electrodes for EDLCs is clearly presented.

Acknowledgements

The present work was supported by the Grant-in-Aid for Scientific Research (No. 22·75 for G.H., No. 22750203 for K.K. and 20350094 for K.N.) from the Ministry of Education, Culture, Sports, Science and Technology (MEXT), Japan. Also acknowledged is the Global COE Program “International Center for Integrated Research and Advanced Education in Materials Science” (No. B-09) of the MEXT, Japan, administrated by the Japan Society for the Promotion of Science (JSPS).

Notes and references

[a] *Department of Chemistry, Graduate School of Science, Kyoto University*

Kitashirakawa, Sakyo-ku, Kyoto 606-8502 Japan. Fax/Tel: +81-75-753-7673*; E-mail:* kanamori@kuchem.kyoto-u.ac.jp

[b] Department of Applied Chemistry, Graduate School of Engineering, Osaka Prefecture University, Sakai, Osaka 599-8531 Japan

† Electronic Supplementary Information (ESI) available: [details of any supplementary information available should be included here]. See DOI: 10.1039/b000000x/

1 Y.-S. Hu, P. Adelhelm, B. M. Smarsly, S. Hore, M. Antonietti, J. Maier, *Adv. Funct. Mater.*, 2007, **17**, 1873.

2 K. M. Thomas, *Catal. Today*, 2007, **120**, 389.

3 E. Frackowiak, F. Béguin, *Carbon*, 2001, **39**, 937.

4 A. G. Pandolfo, A. F. Hollenkamp, *J. Power Sources*, 2006, **157**, 11.

5 P. Simon, Y. Gogotsi, *Nature Mater.*, 2008, **7**, 845.

6 P. Simon, Y. Gogotsi, *Nature Mater.*, 2008, **7**, 845.

7 G. Salitra, A. Soffer, L. Ehad, Y. Cohen, D. Aurbach, *J. Electrochem. Soc.*, 2000, **147**, 2486.

8 O. Barbieri, M. Hahn, A. Herzog, R. Kötz, *Carbon*, 2005, **43**, 1303.

9 W. Xing, S. Z. Qiao, R. G. Ding, F. Li, G. Q. Lu, Z. F. Yan, H. M. Cheng, *Carbon*, 2006, **44**, 216.

10 S. Shiraishi, H. Kurihara, L. Shi, T. Nakayama, A. Oya, *J. Electrochem. Soc.*, 2002, **149**, A855.

11 C. Largeot, C. Portet, J. Chmiola, P. L. Taberna, Y. Gogotsi, P. Simon, *J. Am. Chem. Soc.*, 2008, **130**, 2730.

12 N. Brun, S. R. S. Prabaharan, M. Morcrette, C. Sanchez, G. Pécastaings, A. Derré, A. Soum, H. Deleuze, M. Birot, R. Backov, *Adv. Funct. Mater.*, 2009, **19**, 3136.

13 V. Ruiz, C. Blanco, R. Santamaría, J. M. Ramos-Fernández, M. Martínez-Escandell, A. Sepúlveda-Escribano, F. Rodrígez-Reinoso, *Carbon*, 2009, **47**, 195.

14 J. Lee, S. Yoon, T. Hyeon, S. M. Oh, K. B. Kim, *Chem. Commun.*, 1999, **21**, 2177.

15 S. Álvarez, M. C. Blanco-López, A. J. Miranda-Ordieres, A. B. Fuertes, T. A. Centeno, *Carbon*, 2005, **43**, 855.

16 C. Vix-Guterl, E. Frackowiak, K. Jurewicz, M. Friebe, J. Parmentier, F. Béguin, *Carbon*, 2005, **43**, 1293.

17 W. Xing, S. Z. Qiao, R. G. Ding, F. Li, G. Q. Lu, Z. F. Yan, H. M. Cheng, *Carbon*, 2006, **44**, 216.

18 K. Xia, Q. Gao, J. Jiang, J. Hu, *Carbon*, 2008, **46**, 1718.

19 B. Liu, H. Shioyama, H. Jiang, X. Zhang, Q. Xu, *Carbon*, 2010, **48**, 456.

20 D. W. Wang, F. Li, M. Liu, G. Q. Lu, H. M. Cheng, *Angew. Chem. Int. Ed.*, 2008, **47**, 373.

21 S. W. Woo, K. Dokko, H. Nakano, K. Kanamura, *J. Mater. Chem.*, 2008, **18**, 1674.

22 J. Hasegawa, K. Kanamori, K. Nakanishi, T. Hanada, S. Yamago, *Macromolecules*, 2009, **42**, 1270.

23 J. Hasegawa, K. Kanamori, K. Nakanishi, T. Hanada, *C. R. Chimie*, 2010, **13**, 207.

24 G. Hasegawa, K. Kanamori, K. Nakanishi, T. Hanada, *Carbon*, 2010, **48**, 1757.

25 D. Hulicova, J. Yamashita, Y. Soneda, H. Hatori, M. Kodama, *Chem. Mater.*, 2005, **17**, 1241.

26 K. Jurewicz, K. Babel, A. Źiółkowski, H. Wachowska, *Electrochim. Acta*, 2003, **48**, 1491.

27 N. D. Kim, W. Kim, J. B. Joo, S. Oh, P. Kim, Y. Kim, J. Yi, *J. Power Sources*, 2008, **180**, 671.

28 W. S. Baker, J. W. Long, R. M. Stroud, D. R. Rolison, *J. Non-Cryst. Solids*, 2004, **350**, 80.

29 J. W. Neely, *Carbon*, 1981, **19**, 27.

30 H. G. M. Edwards, D. R. Brown, J. R. Dale, S. Plant, *Vib. Spectrosc.*, 2000, **24**, 213.

31 D. Hines, A. Bagreev, T. J. Bandosz, *Langmuir*, 2004, **20**, 3388.

32 M. Toyoda, U. Tani, Y. Soneda, *Carbon*, 2004, **42**, 2833.

33 Y. T. Kim, T. Mitani, *J. Power Sources*, 2006, **158**, 1517.

34 D. Hulicova-Jurcakokova, M. Kodama, S. Shiraishi, H. Hatori, Z. H. Zhu, G. Q. Lu, *Adv. Funct. Mater.*, 2009, **19**, 1800.